



1 An upward continuation method based on spherical harmonic 2 analysis and its application in the calibration of satellite gravity 3 gradiometry data

4 Qingliang Qu^{1,2}, Shengwen Yu¹, Guangbin Zhu², Xiaotao Chang², Miao Zhou^{1,2}, and Wei Liu²

5 ¹ College of Geomatics, Shandong University of Science and Technology, Qingdao 266510, China.

6 ² Land Satellite Remote Sensing Application Center of the Ministry of Natural Resources, Beijing 100048,
 7 China.

8 Correspondence to: Shengwen Yu (sdkdswwy@163.com)

9 **Abstract.** The ground gravity anomalies can be used to calibrate and validate the satellite gravity gradiometry
 10 data. In this study, an upward continuation method of ground gravity data based on spherical harmonic analysis
 11 is proposed, which can be applied to the calibration of satellite observations from the European Space Agency's
 12 Gravity Field and Steady-State Ocean Circulation Explorer (GOCE). Here, the following process was conducted
 13 to apply this method. The accuracy of the upward continuation method based on spherical harmonic analysis was
 14 verified using simulated ground gravity anomalies. The DTU13 global gravity anomaly data were used to
 15 determine the calibration parameters of the GOCE gravitational gradients based on the spherical harmonic
 16 analysis method. The trace and the tensor invariants I_2 , I_3 of the gravitational gradients were used to verify the
 17 calibration results. The results revealed that the upward continuation errors based on spherical harmonic analysis
 18 were much smaller than the noise level in the measurement bandwidth of the GOCE gravity gradiometer. The
 19 scale factors of the V_{xx} , V_{yy} , V_{zz} , and V_{yz} components were determined at an order of magnitude of approximately
 20 10^{-2} , the V_{xz} component was approximately 10^{-3} , and the V_{xy} component was approximately 10^{-1} . The traces of
 21 gravitational gradients after calibration were improved when compared with the traces before calibration and were
 22 slightly better than the EGG_TRF_2 data released by the European Space Agency (ESA). In addition, the relative
 23 errors of the tensor invariants I_2 , I_3 of the gravitational gradients after calibration were significantly better than
 24 those before calibration. In conclusion, the upward continuation method based on spherical harmonic analysis
 25 could meet the external calibration accuracy requirements of the gradiometer.

26 1 Introduction

27 The European Space Agency's Gravity Field and Steady-State Ocean Circulation Explorer (GOCE) satellite was
 28 launched on 17 March 2009. The goals of the mission were the retrieval of the global geoid model with 1–2 cm
 29 accuracy and the determination of the global gravity anomalies with 1 mGal accuracy for a spatial resolution of
 30 100 km or less (Drinkwater et al., 2006; Bouman and Fuchs, 2012; van der Meijde et al., 2015; Bouman et al.,
 31 2016; Siemes, 2018). To achieve these goals, the GOCE satellite combined the satellite gravity gradiometry (SGG)
 32 technique with satellite-to-satellite tracking in the high-low mode (SST–hl). The SST technique is sensitive to the
 33 long wavelength signals of the Earth's gravitational field and the SGG technique can contribute to obtaining the
 34 medium and short wavelength signals of the Earth's gravitational field. The electrostatic gravity gradiometer
 35 mounted on the GOCE satellite can measure the second derivative of the Earth's gravitational potential with high
 36 precision. This gradiometer, however, is bandwidth limited to 0.005–0.1 Hz. Therefore, the gravitational gradient
 37 observations may still suffer from system errors, such as scale factors and biases. In this case, an external



calibration strategy is needed to achieve high-precision gravity gradiometry data. In general, the existing Earth gravitational models, ground gravity data, and SST observations are used to perform the external calibration of the GOCE gravitational gradients. The calibration of GOCE gravitational gradients using ground gravity data will be examined and outlined here.

Arabelos and Tscherning (Arabelos and Tscherning, 1998) described a simulation study of the external calibration approach for SGG data with ground gravity data and used the least-squares collocation (LSC) method to detect the systematic errors of gravitational gradients. The a priori covariance relationship of the upward continuation of ground gravity data onto gravitational gradients was discussed in Bouman et al. and Pail (Pail, 2002; Bouman and Koop, 2003). Denker (Denker, 2002) applied the least squares spectral combination technique to the upward continuation of the ground gravity data onto gravitational gradients at satellite altitude. It was proven that the accuracy of this method can reach a few mE ($1 \text{ mE} = 10^{-12}/\text{s}^2$). Two methods for the upward continuation of ground gravity data onto gravitational gradients, namely, the LSC and integral formula methods based on the spectral combination technique, were discussed and compared in Wolf and Denker (Wolf and Denker, 2005). A synthetic geopotential model, which combined the GRACE geopotential model, EGM96 geopotential model, and GPM98C geopotential model, was used to simulate the gravity anomalies on terrain and on an ellipsoid. This study revealed that the results of the two methods were similar and the accuracies of six components were 0.1–0.6 mE and 0.3–1.4 mE, respectively, when the gravity anomalies on the terrain and ellipsoid were applied for the continuation. The integral formulas based on the extended Stokes and Hotine formulas were used by Kern and Haagmans (Kern and Haagmans, 2005) to determine all the components of the gravitational gradients from terrestrial gravity data. They found that the difference between the computed gravitational gradients and the model values from the GPM98A geopotential model ranged from 1.5 to 2.5 mE for all components. To validate the SGG data, an external calibration model based on the regional ground gravity data was described in Bouman et al. (Bouman et al., 2004; Bouman et al., 2009; Bouman et al., 2011). The results showed that the scale factors of the gradiometer can be determined at the 10^{-2} level using the LSC upward continuation method, and that ground gravity data can be used to validate the measured and calibrated gravitational gradients. A least squares modification of the extended Stokes formula and its second-order radial derivative was proposed by Eshagh (Eshagh, 2010). This method was used to generate the gravitational gradients at satellite altitude from the ground gravity data to validate the SGG data. The airborne gravity data of the Antarctic region were applied to validate the GOCE gravity gradiometry data in Yildiz et al. (Yildiz, 2012; Yildiz et al., 2016). They concluded that the differences between the calculated gravitational gradients from the LSC upward continuation method and the GOCE gravitational gradient observations were 9.9 mE, 11.5 mE, 11.6 mE, and 10.4 mE in the high-precision components V_{xx} , V_{yy} , V_{zz} , and V_{xz} , respectively. The validation of the V_{zz} component of the GOCE gravitational gradients by geoidal undulation using semi-stochastic modifications of the Abel-Poisson integral was discussed in Eshagh (Eshagh, 2011). Šprlák et al. (Šprlák et al., 2015) presented new integral transforms of the gravitational potential disturbances derived from satellite altimetry data onto the gravitational gradients at satellite altitude. Thus, we see that the LSC and integral formula methods are commonly used in the upward continuation of the ground gravity data onto the gravitational gradients at satellite altitude for the calibration of SGG data. The key to applying the LSC method is to construct the covariance functions between the gravity anomalies and the gravitational gradients. The inverse matrix of the large covariance matrix is very difficult to solve in massive data



processing, however. The calculation of the transformation kernel function in the integral formula method is relatively complicated, and the influence of the boundary effect should be considered. In this article, we discuss the possibilities of spherical harmonic analysis for the upward continuation of the ground gravity data onto the gravitational gradients at satellite altitude. The upward continuation method based on spherical harmonic analysis is more convenient to use than the LSC and integral formula methods. In addition, the DTU13 gravity anomalies were used to calibrate the GOCE SGG data based on this method.

2 Methods

2.1 Upward continuation method based on the spherical harmonic analysis

A square integrable function $f(\theta, \lambda)$ defined on the unit sphere can be expanded into a series of spherical harmonics as (Colombo, 1981; Kern, 2003):

$$f(\theta, \lambda) = \sum_{n=0}^{\infty} \sum_{m=0}^n [\bar{C}_{nm} \cos m\lambda + \bar{S}_{nm} \sin m\lambda] \bar{P}_{nm}(\cos \theta), \quad (1)$$

where θ, λ are the geocentric co-latitude and longitude of the computation point, respectively, \bar{P}_{nm} is the fully normalized Legendre polynomial of degree n and order m , and \bar{C}_{nm} and \bar{S}_{nm} denote the fully normalized gravity field harmonic and Stokes coefficients, respectively.

The purpose of spherical harmonic analysis is to estimate the coefficients \bar{C}_{nm} and \bar{S}_{nm} based on the function $f(\theta, \lambda)$, which is the inverse process of spherical harmonic synthesis. Therefore, the coefficients can be obtained using:

$$\left\{ \begin{array}{l} \bar{C}_{nm} \\ \bar{S}_{nm} \end{array} \right\} = \frac{1}{4\pi} \int_{\sigma} f(\theta, \lambda) \left\{ \begin{array}{l} \cos m\lambda \\ \sin m\lambda \end{array} \right\} \bar{P}_{nm}(\cos \theta) d\sigma, \quad (2)$$

where $d\sigma$ is the grid area and $d\sigma = \sin \theta d\theta d\lambda$. In general, the function $f(\theta, \lambda)$ is unknown, but we can obtain the values of each grid point or the average values over the grid areas. Thus, Equation (2) can be discretized as:

$$\left\{ \begin{array}{l} \bar{C}_{nm} \\ \bar{S}_{nm} \end{array} \right\} = \frac{1}{4\pi} \sum_{i=1}^N \sum_{j=1}^{2N} f(\theta_i, \lambda_j) \left\{ \begin{array}{l} \cos m\lambda_j \\ \sin m\lambda_j \end{array} \right\} \bar{P}_{nm}(\cos \theta_i) \sin \theta_i \Delta_{ij}, \quad (3)$$

where $\Delta_{ij} = \Delta\theta \cdot \Delta\lambda$ and $\Delta\theta = \Delta\lambda$ when the grid is regular, and N is the number of latitude grid points.

In this study, the spherical harmonic analysis of gravity anomalies was needed. The gravity anomaly can be computed as:

$$\Delta g = \frac{GM}{r^2} \sum_{n=2}^{n_{max}} \sum_{m=0}^n \left(\frac{R}{r} \right)^n (n-1) \left(\bar{C}_{nm}^* \cos m\lambda + \bar{S}_{nm} \sin m\lambda \right) \bar{P}_{nm}(\cos \theta), \quad (4)$$

where Δg is the gravity anomaly, M is the mass of the Earth, G is the gravitational constant, R is the mean equatorial radius, r is the geocentric radius, and \bar{C}_{nm}^* is the spherical harmonic coefficients from which the normal ellipsoid gravitational potential coefficients have been subtracted.

Combining Equations (3) and (4), the point values of the spherical harmonic analysis expression of the gravity anomaly can be derived as:



$$\left. \begin{matrix} \bar{C}_{nm}^* \\ \bar{S}_{nm} \end{matrix} \right\} = \frac{r^2}{4\pi GM(n-1)} \left(\frac{r}{R} \right)^n \sum_{i=1}^N \sum_{j=1}^{2N} \Delta g(\theta_i, \lambda_j) \sin \theta_i \Delta_{ij}. \quad (5)$$

The fully normalized gravity field harmonic coefficients \bar{C}_{nm} can be obtained by adding the normal ellipsoid gravitational potential coefficients to \bar{C}_{nm}^* . Combining with the precise scientific orbit data of the GOCE, the ground gravity anomalies can be upwardly continued onto the gravitational gradients at satellite altitude in the local north-oriented frame (LNOF), where the x-axis points to the north, the y-axis east, and the z-axis radially outward (Figure 1).

2.2 External calibration method

The calibration using ground gravity data relies on the comparison of the GOCE gravitational gradients and the upward continuation gravitational gradients. The GOCE gravitational gradients from the EGG_NOM_2 data are presented in the gradiometer reference frame (GRF), where the x-axis is parallel to the instantaneous direction of the orbital velocity vector, and the y-axis is parallel to the instantaneous direction of the orbital angular momentum (Figure 1). The upward continuation gradients are generally expressed in the LNOF, however. Therefore, frame transformation is required during the external calibration process. When the gravitational gradients in the LNOF are converted to the GRF, several coordinate rotation steps are necessary. The model of the frame transformation is:

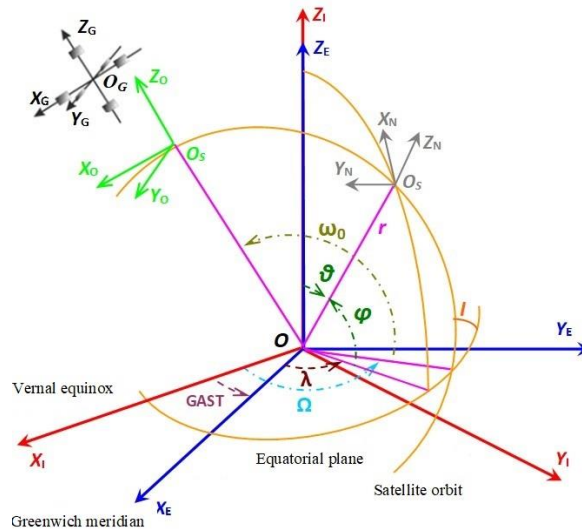
$$\mathbf{V}_{GRF} = \mathbf{R} \mathbf{V}_{LNOF} \mathbf{R}^T, \quad (6)$$

where \mathbf{R} is the transformation matrix, such that $\mathbf{R} = \mathbf{R}_{EFRF}^{LNOF} \cdot \mathbf{R}_{IRF}^{EFRF} \cdot \mathbf{R}_{GRF}^{IRF}$ (Fuchs and Bouman, 2011). \mathbf{R}_{EFRF}^{LNOF} is the transformation matrix from the LNOF to the Earth-fixed reference frame (EFRF) system, where the x-axis is fixed in the equatorial plane in the direction of the Greenwich meridian, and the z-axis is the direction of the pole (Figure 1); \mathbf{R}_{IRF}^{EFRF} is the transformation matrix from the EFRF to the inertial reference frame (IRF), where the x-axis is fixed in the equatorial plane in the direction of the vernal equinox, and the z-axis is the direction of the pole (Figure 1); and \mathbf{R}_{GRF}^{IRF} is the transformation matrix from the IRF to the GRF.

The calibration parameters of the GOCE gravitational gradients were determined as follows:

$$V_{ij}^m(t) = \lambda V_{ij}^s(t) + b \quad i, j = x, y, z, \quad (7)$$

where V_{ij}^m are the upward continuation values, V_{ij}^s are the GOCE gradiometry observations, λ is the scale factor, b is the bias, and t is the time. Least squares estimation was then used to estimate the parameters.



133

134 Figure 1. Reference systems for the GOCE satellite: $O_G - X_G Y_G Z_G$ is the GRF coordinate system, $O_S - X_N Y_N Z_N$ is the
 135 LNOF coordinate system, $O - X_I Y_I Z_I$ is the IRF coordinate system, and $O - X_E Y_E Z_E$ is the EFRF coordinate system.

136 3 Results and Discussion

137 3.1 Accuracy of the upward continuation method

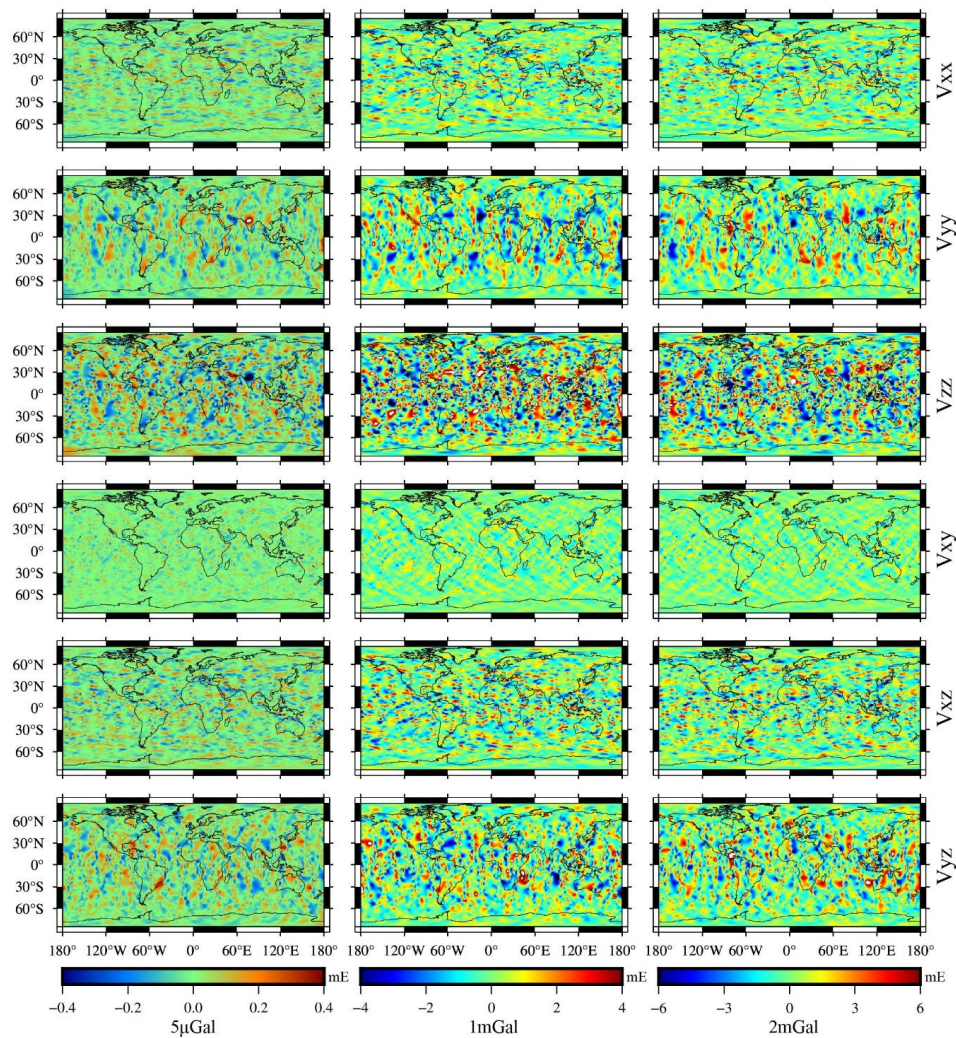
138 The accuracy of the upward continuation method based on spherical harmonic analysis was verified by simulation.
 139 The high-precision global gravity field model EGM2008 (Pavlis et al., 2008) was selected for the computation.
 140 The precise orbital data of the GOCE with a time interval of 1 s from 11 February 2011 to 17 February 2011 were
 141 used to compute the gravitational gradients at satellite altitude. Hence, the total number of observations was
 142 604,800. The verification schemes were designed as follows.

143 Scheme 1. The grid gravity anomalies Δg^{true} with a resolution of 0.5° on the sphere calculated by the EGM2008
 144 field to degree and order 360 were regarded as the simulated ground gravity data. Next, combining with the precise
 145 orbit data, the simulated ground gravity data Δg^{true} were upwardly continued onto the gravitational gradients
 146 $V_{ij}^0 (i, j = x, y, z)$ at the satellite altitude based on spherical harmonic analysis. Finally, the upward continuation
 147 gravitational gradients V_{ij}^{true} were compared with the gravitational gradients directly calculated by the EGM2008
 148 field. The upward continuation errors based on spherical harmonic analysis could be obtained using this scheme.
 149 Scheme 2. The gravity anomalies Δg^{true} were added to 5 μGal , 1 mGal and 2 mGal white noise, serving as the
 150 ground-truth measurement data. The remaining steps were the same as scheme 1. The influence of the accuracy
 151 of ground gravity anomalies on upward continuation errors could be obtained by this scheme.

152 Figure 2 shows the spatial distribution of upward continuation errors using different ground gravity accuracy in
 153 scheme 2. There is no general pattern can be observed, indicating that the upward continuation errors were



154 randomly distributed over the orbits. When the accuracy of the ground gravity anomalies was 5 μGal , the
 155 differences between the upward continuation gravitational gradients and the gravitational gradients calculated by
 156 the EGM2008 field for all of the components ranged from -0.4 to 0.4 mE. When the accuracy of the ground gravity
 157 anomalies was 1 mGal and 2 mGal, the differences mostly varied from -4 to 4 mE and -6 to 6 mE. Therefore, the
 158 accuracy of the ground gravity anomalies exerted a significant influence on the upward continuation errors. Table
 159 1 lists the statistics of the upward continuation errors in each component of the gravitational gradients for the
 160 different schemes. The accuracy of the upward continuation of the V_{zz} component was lower than that of the other
 161 components. When there was no noise in the gravity anomalies (scheme 1), the errors caused by the upward
 162 continuation method based on spherical harmonic analysis were 10^{-3} mE in the V_{xx} , V_{yy} , V_{zz} , and V_{xz} components
 163 and 10^{-5} mE in the V_{xy} and V_{yz} components. Meanwhile, the noise level was approximately 5–8 mE in the
 164 measurement bandwidth of the gravity gradiometer (Rummel et al., 2011). Thus, it can be seen that the upward
 165 continuation errors were far less than the noise level in the measurement bandwidth of the gradiometer. When the
 166 gravity anomalies contained 5 μGal of white noise, the standard deviations of the upward continuation errors of
 167 the V_{xx} , V_{yy} , V_{xy} , V_{xz} , and V_{yz} components were 10^{-2} mE and 0.1 mE in the V_{zz} component, which were still
 168 significantly lower than the noise level in the measurement bandwidth of the gravity gradiometer. When the
 169 gravity anomalies contained 1 mGal or 2 mGal of white noise, the standard deviations of the upward continuation
 170 errors of all components ranged from 0.5 to 1.6 mE, which was also less than the noise level in the measurement
 171 bandwidth of the gravity gradiometer. This indicates that the upward continuation method for gravity anomalies
 172 of gravitational gradients based on spherical harmonic analysis can be used to calibrate the SGG data. Moreover,
 173 if the ground data are more accurate, then the gravitational gradients at the satellite altitude obtained by upward
 174 continuation will also be more accurate.



175

176

177

178

Figure 2. Distribution of upward continuation errors of the gravitational gradients using ground gravity data.

Table 1. Standard deviation of upward continuation errors in gravitational gradients for different simulation schemes (mE).

Component		V_{xx}	V_{yy}	V_{zz}	V_{xy}	V_{xz}	V_{yz}
Scheme 1		1.4×10^{-3}	1.0×10^{-3}	2.5×10^{-3}	2.8×10^{-5}	1.7×10^{-3}	4.6×10^{-5}
Scheme 2	5 μ Gal	7.2×10^{-2}	7.2×10^{-2}	1.0×10^{-1}	4.0×10^{-2}	8.3×10^{-2}	8.3×10^{-2}
	1 mGal	0.8	0.8	1.2	0.5	1.0	1.0
	2 mGal	1.0	1.0	1.6	0.7	1.3	1.3



3.2 Calibration results with DTU13 global gravity anomalies

Compared with the global gravity field model, the DTU13 (Andersen et al., 2014; Andersen et al., 2015) gravity anomalies contain more high frequency signals, and its accuracy is about 2 mGal. Therefore, the DTU13 global gravity anomalies with a resolution of 0.5° were applied in the numerical experiment to calibrate the gravitational gradients of the GOCE satellite. The DTU13 global gravity anomalies are shown in Figure 3. To reduce the influence of the long wavelength signals of the gravitational field, the remove-restore procedure was applied based on the reference geopotential model EGM2008 up to degree and order 360. The upward continuation of the residual gravity was extended to the satellite altitude using the spherical harmonic analysis method, and the long wavelength signals of the gravity field were then restored. The GOCE data used in this study spanned the period February 11 to June 23, 2011, with a time interval of 1 s. Referring to Bouman et al. (Bouman et al., 2011), the calibration period was set to 7 days. Hence, the data were divided into 19 weeks.

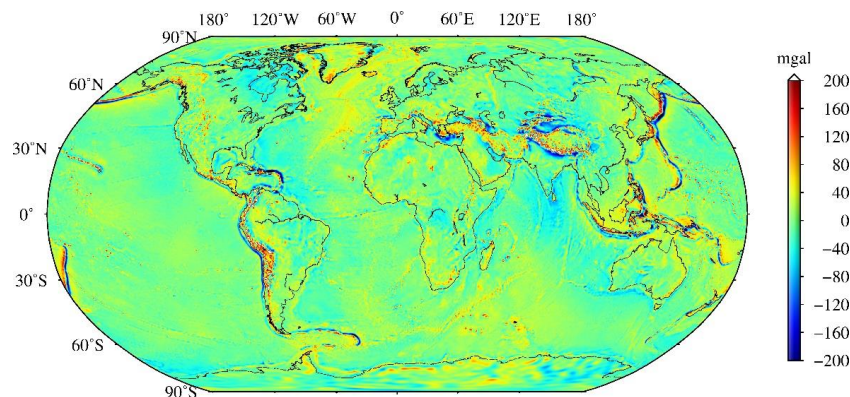
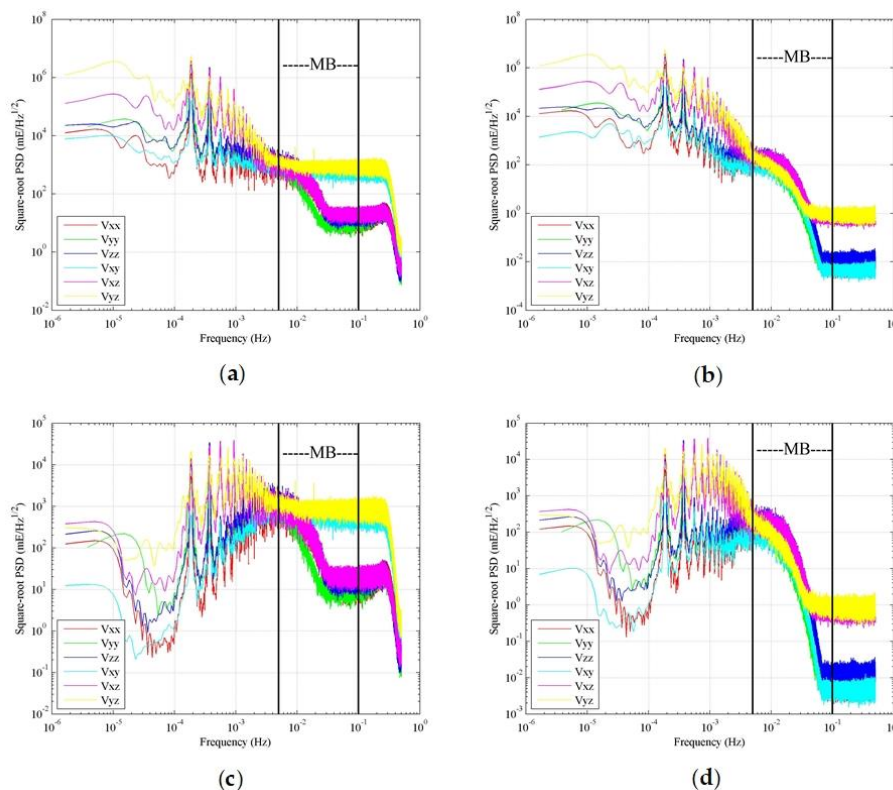


Figure 3. Global gravity anomalies of the DTU13.

Corrections for temporal gravity field variations and outlier detection of the GOCE gravitational gradients were conducted in the EGG_NOM_2 file. The outliers were replaced by cubic spline interpolation values in this study. The power spectral density (PSD) of the GOCE gravitational gradients and the upward continuation values from the ground gravity anomalies are displayed in Figures 4(a) and (b). Because of the measurement bandwidth limitation of the gravity gradiometer, the noise of the gravitational gradients was large below the lower limit of the measurement bandwidth, which exhibited a $1/f$ behavior. Therefore, a second-order high-pass Butterworth filter was adopted before calibration. Various filter cut-off frequencies were discussed in Bouman et al. (Bouman et al., 2011). They pointed out that the cut-off frequencies of 3, 5, and 7 mHz are appropriate for GOCE SGG data. Therefore, 3 mHz was used as the cut-off frequency in this study, which was below the lower bound of the measurement bandwidth and retained more gravitational gradient signals of the GOCE SGG data. Figures 4(c) and (d) are the filtered signals of the GOCE gravitational gradients and the upward continuation values. It is clear that the effect of low frequency signals was suppressed, although the noise level was still high when the frequency was close to the lower limit of the measurement bandwidth. When the frequency was between 0.005 Hz and 0.03 Hz, the GOCE gravitational gradients in the V_{xx} , V_{yy} , V_{zz} , and V_{xz} components decreased rapidly, while the V_{xy} and V_{yz} components remain a constant about 10^3 mE. Meanwhile, the upward continuation values decreased rapidly



207 in all six components. When the frequency was between 0.03 Hz and 0.1 Hz, the V_{xx} , V_{yy} , V_{zz} , and V_{xz} components
 208 decreased to 10–20 mE for the GOCE gravitational gradients, although the V_{xx} , V_{yy} , V_{zz} , and V_{xy} components
 209 decreased to approximately 10^{-2} mE and the V_{xz} , V_{yz} components decreased to approximately 1 mE for the upward
 210 continuation values.



211
 212 Figure 4. Power spectral density of gravitational gradients: (a) GOCE observations; (b) upward continuation
 213 values; (c) GOCE observations after high-pass filtering; (d) upward continuation values after high-pass filtering.
 214 Figures 5 and 6 reflect the changes of the scale factors and biases for the GOCE gravitational gradients. It appears
 215 that the scale factors had a period of approximately 3 weeks, which corresponds to the 20-day subcycle of the
 216 GOCE satellite orbit. After high-pass filtering, the biases were very small, with maxima on the order of 10^{-5} for
 217 all components of the GOCE gravitational gradients. Table 2 lists the statistics of the scale factors for the six
 218 components of the gravitational gradients. The deviations between the mean values of the scale factors and one
 219 ranged from approximately 0.02 to 0.03 for the diagonal components. These results are larger than those of
 220 Veicherts et al. (Veicherts et al., 2011) for Australia, Canada, and parts of Scandinavia, but smaller than those of
 221 the Norway area. The reason for these differences is that, on the one hand, the accuracy levels of the DTU13
 222 gravity anomalies and the regional ground gravity data used in the Veicherts study are different. On the other
 223 hand, the calibration parameters are determined globally rather than in a certain area. The stability of the scale



224 factors for the diagonal components had a magnitude of approximately 10^{-2} , while the ultra-sensitive component
 225 V_{xz} was the best, reaching a magnitude of 10^{-3} . In contrast, the stability of the scale factor for the V_{xy} component
 226 was poor, only about 10^{-1} . Given the scale factors derived from the comparison between the filtered upward
 227 continuation gravitational gradients and the filtered GOCE gravitational gradients, the upward continuation
 228 gravitational gradients were regarded as the true values. The V_{xy} component exhibited the maximum difference
 229 between the GOCE gravitational gradients and the upward continuation values within the measurement bandwidth,
 230 as seen in Figures 4(c) and (d). In other words, the noise level was highest in the V_{xy} component, so the scale
 231 factors of this component were unstable. This phenomenon is also consistent with the design characteristics of the
 232 GOCE gravity gradiometer.

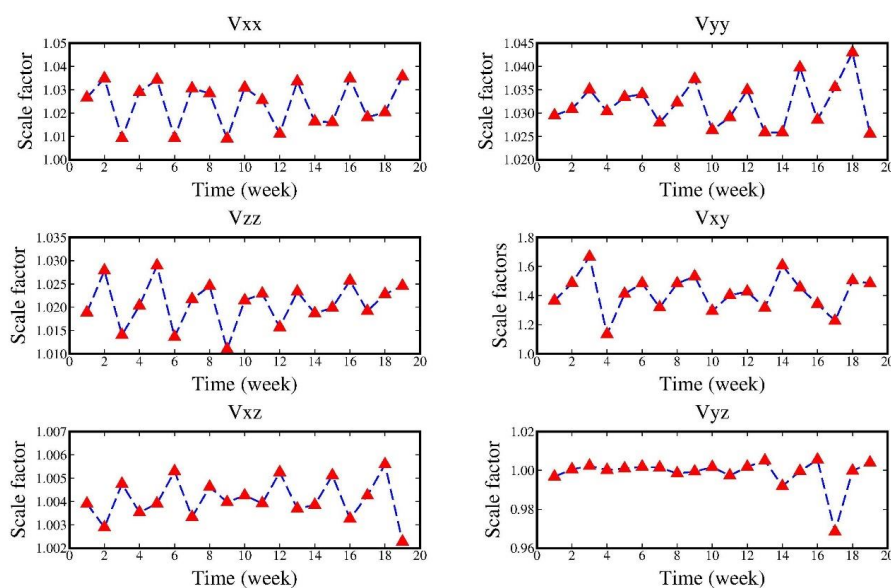


Figure 5. Variations of scale factors during the calibration period.

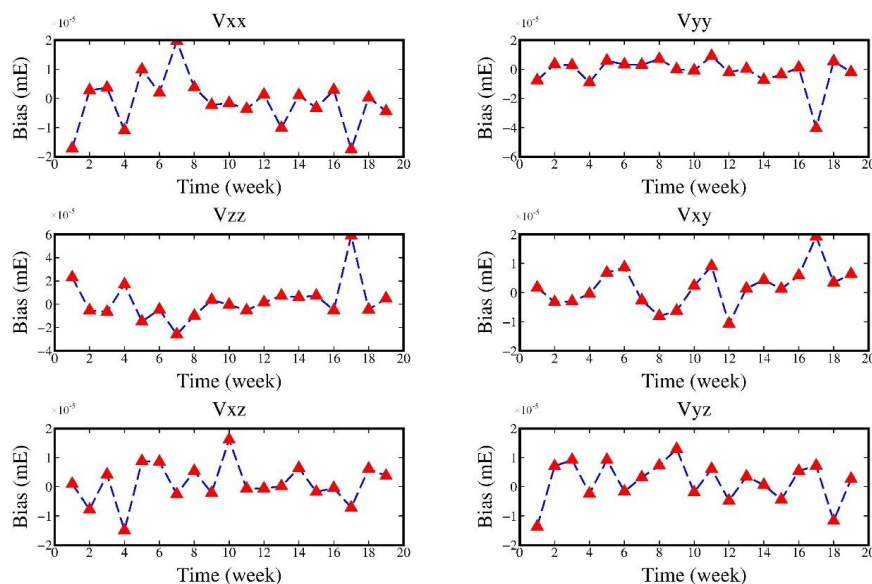


Figure 6. Variations of biases during the calibration period.

Table 2. Statistics of the scale factors.

Component	Minimum	Maximum	Mean	Standard deviation
V_{xx}	1.0090	1.0357	1.0239	9×10^{-3}
V_{yy}	1.0256	1.0430	1.0318	5×10^{-3}
V_{zz}	1.0110	1.0290	1.0208	5×10^{-3}
V_{xy}	1.1348	1.6660	1.4177	1×10^{-1}
V_{xz}	1.0023	1.0056	1.0041	8×10^{-4}
V_{yz}	0.9684	1.0055	0.9988	8×10^{-3}

4 Discussion of the calibration results

After the calibration of the GOCE gravitational gradients was completed, the calibration results needed to be verified and analyzed to ensure the calibration accuracy, which was key to checking the quality of the gravitational gradients of the GOCE satellite.

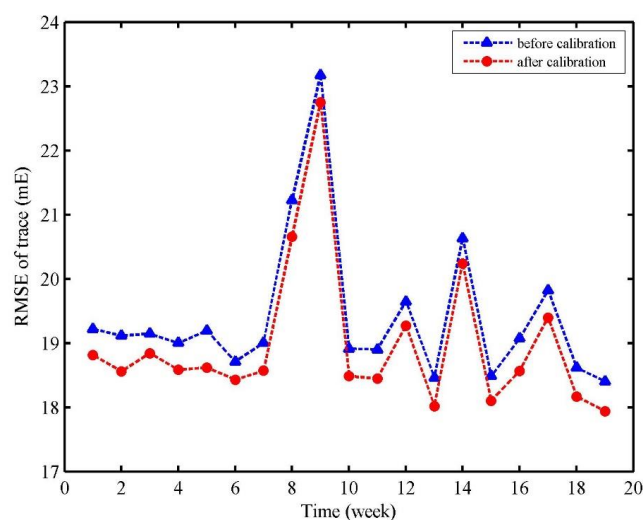
(1) Verification by the trace-free characteristics of gravitational gradients

The gravitational gradients satisfy the Laplace equation in the space around the Earth, i.e., the trace of the gravitational gradient observations is 0. Based on this criterion, the calibration results were verified and evaluated.

The calibration parameters were applied to the high-pass-filtered SGG observations, after which the trace of the gravitational gradients following calibration could be obtained. Figure 7 displays the root mean square error of the trace of the gravitational gradients in the 19 weeks after calibration. It is obvious that the trace of the GOCE gravitational gradients improved after calibration. During the calibration period, the maximum value appeared in the ninth week, at which point it was approximately 23.2 mE before calibration and approximately 22.7 mE after



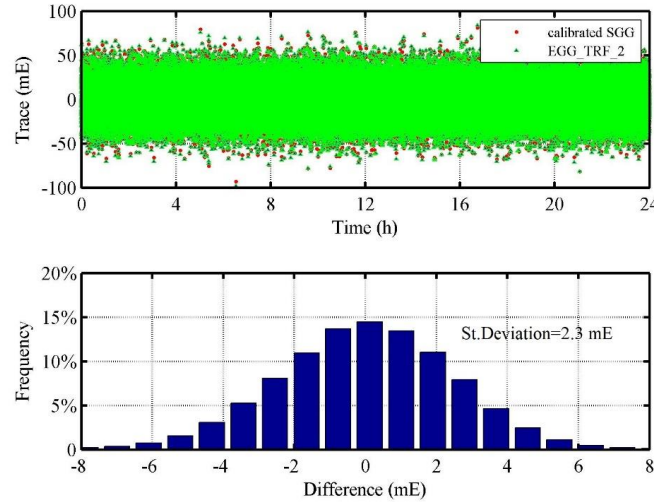
250 calibration. Although the GOCE satellite was not offline and its onboard system was operating normally at that
 251 time, a large number of GOCE gravitational gradient data were still missing. This phenomenon may be related to
 252 changes in the external space environment of the electrostatic gravity gradiometer, such as solar and geomagnetic
 253 activities.



254

255 Figure 7. Root mean square error of the trace of the gravitational gradients before and after calibration.

256 In addition, the calibrated gravitational gradients in the EGG_TRF_2 (ESA, 2014) were used to verify the results.
 257 The EGG_TRF_2 observations were transferred from the LNOF to the GRF and filtered by the same high-pass
 258 filter described in Section 3.2. The time-dependent change of the trace between the calibrated GOCE gravitational
 259 gradients and the EGG_TRF_2 observations, along with the histogram of residuals in 1 day, are shown in Figure
 260 8. From a time series perspective, the trace of the calibrated GOCE gravitational gradients was consistent with
 261 the EGG_TRF_2 data. The histogram shows that 95% of the differences between the calibrated GOCE
 262 gravitational gradients and the EGG_TRF_2 observations were within 5 mE and the standard deviation of the
 263 residuals was approximately 2.3 mE. The standard deviation of the trace of the calibrated gradiometry
 264 observations in this study was approximately 18.6 mE, whereas the EGG_TRF_2 was approximately 18.9 mE.
 265 This indicates that the accuracy of the calibration results of the gravitational gradients based on spherical harmonic
 266 analysis was slightly better than that of the EGG_TRF_2 data.



267

268 Figure 8. Comparison of the trace of the calibrated gravitational gradients with the trace of the EGG_TRF_2.

269 (2) Verification by the tensor invariants method

270 Because the trace criterion can only verify the overall accuracy of the calibrated diagonal components of the
 271 gravitational gradients, the tensor invariants were introduced into the accuracy verification process. Combined
 272 with the prior gravity field model information, the independent accuracy verification of the diagonal component
 273 and the non-diagonal component of the gravitational gradients could be realized.

274 The application of 3 tensor invariants in the verification of the gravitational gradients can be expressed as (Baur
 275 et al., 2008; Lu et al., 2018):

$$276 \quad \begin{cases} I_1 = V_{xx} + V_{yy} + V_{zz} \\ I_2 = -\frac{1}{2} V_{xx}^2 + V_{yy}^2 + V_{zz}^2 - V_{xy}^2 - V_{xz}^2 - V_{yz}^2 \\ I_3 = V_{xx} V_{yy} V_{zz} + 2V_{xy} V_{xz} V_{yz} - V_{xx} V_{yz}^2 - V_{yy} V_{xz}^2 - V_{zz} V_{xy}^2 \end{cases} \quad (8)$$

277 It is clear that the tensor invariant I_1 is the trace of the gravitational gradients, which was utilized before. The
 278 tensor invariants I_2 and I_3 comprise all six components of the gravitational gradients, and their relative error before
 279 and after calibration (Equation [9]) could be used to evaluate the calibration results,

$$280 \quad \begin{aligned} \delta_2^o &= \frac{|I_2^o - I_2^r|}{I_2^r} \times 100\% \\ \delta_2^c &= \frac{|I_2^c - I_2^r|}{I_2^r} \times 100\% \\ \delta_3^o &= \frac{|I_3^o - I_3^r|}{I_3^r} \times 100\% \\ \delta_3^c &= \frac{|I_3^c - I_3^r|}{I_3^r} \times 100\% \end{aligned} \quad (9)$$



281 The superscripts o , c , and r represent the GOCE gravitational gradient observations, the calibrated gravitational
 282 gradient values, and the model values calculated by the EGM2008 gravitational potential model up to degree and
 283 order 360, respectively. Here, the calibrated gravitational gradient values indicate that the signals below 3 mHz
 284 were replaced by the signals from the EGM2008 gravitational potential model up to degree and order 360.
 285 Therefore, δ_2^o, δ_3^o are the tensor invariants I_2, I_3 before calibration, whereas δ_2^c, δ_3^c are the tensor invariants
 286 I_2, I_3 after calibration.
 287 The statistics for the relative errors of the tensor invariants I_2, I_3 before and after calibration in the first calibration
 288 period are listed in Table 3. For the V_{xx}, V_{yy}, V_{zz} , and V_{xz} components, the relative errors of the tensor invariants
 289 I_2, I_3 after calibration were 2–4 orders of magnitude smaller than those before calibration. For the less accurate
 290 components V_{xy} and V_{yz} , the effects of calibration were more apparent. This indicates that the calibration result of
 291 the upward continuation method based on spherical harmonic analysis was effective when the tensor invariant I_2
 292 or I_3 was used to verify the calibration accuracy.

Table 3. Relative errors of tensor invariant I_2 (%).

Component		V_{xx}	V_{yy}	V_{zz}	V_{xy}	V_{xz}	V_{yz}
Invariant I_2	Before calibration	3.1×10^{-2}	0.2	4.2×10^{-2}	1.7	1.6×10^{-2}	156.1
	After calibration	1.6×10^{-4}	1.5×10^{-4}	3.7×10^{-4}	3.8×10^{-6}	5.7×10^{-6}	3.3×10^{-4}
Invariant I_3	Before calibration	0.2	0.3	3.4×10^{-2}	4.95	2.4×10^{-2}	227.65
	After calibration	4.9×10^{-4}	4.5×10^{-4}	2.8×10^{-4}	9.8×10^{-6}	8.5×10^{-6}	5.0×10^{-4}

294 5 Conclusions

295 Based on the spherical harmonic analysis method, the gravitational gradients at the altitude of the GOCE satellite
 296 were calculated using the simulated ground gravity anomaly data, and verification was performed. The external
 297 calibration parameters of the GOCE gravitational gradients were determined using DTU13 global gravity
 298 anomalies.
 299 The simulation process verified the accuracy and application potential for calibrating the satellite gravity
 300 gradiometry data using the spherical harmonic analysis method. The results revealed that the upward continuation
 301 errors were smaller than the noise level in the measurement bandwidth of the gravity gradiometer.
 302 After calibrating the GOCE gravitational gradients with the DTU13 ground gravity data, the stability of the scale
 303 factors in the V_{xx}, V_{yy}, V_{zz} , and V_{yz} components had a magnitude of approximately 10^{-2} , and approximately 10^{-3} in
 304 the V_{xz} component, whereas the stability of the V_{xy} component had a magnitude of only 10^{-1} . The reliability of the
 305 calibration results was verified through the gravitational gradients trace and the tensor invariants method. The
 306 trace of the gravitational gradients after calibration was smaller than before calibration, with an average value of
 307 18.6 mE after calibration, which was slightly better than the accuracy of the EGG_TRF_2 data. The relative errors
 308 of the tensor invariants I_2, I_3 after calibration were 2–4 orders of magnitude smaller than the errors before
 309 calibration.



Data Availability: The satellite gravity gradiometry data used in this study are available from <https://goce-ds.eo.esa.int/oads/access/collection> and the DTU13 gravity anomaly data are available from <ftp://ftp.spacecenter.dk/pub/>.

Conflicts of Interest: The authors declare that there are no conflicts of interest regarding the publication of this paper.

Author Contributions: Conceptualization, Qingliang Qu, Guangbin Zhu and Xiaotao Chang; methodology, Qingliang Qu and Guangbin Zhu; software, Qingliang Qu; validation, Qingliang Qu; formal analysis, Qingliang Qu; investigation, Qingliang Qu; resources, Miao Zhou and Wei Liu; data curation, Miao Zhou and Wei Liu; writing–original draft preparation, Qingliang Qu; writing–review and editing, Shengwen Yu, Guangbin Zhu and Xiaotao Chang; visualization, Shengwen Yu, Guangbin Zhu and Xiaotao Chang; supervision, Shengwen Yu, Guangbin Zhu and Xiaotao Chang; project administration, Guangbin Zhu; funding acquisition, Guangbin Zhu. All authors have read and agree to the published version of the manuscript.

Funding Statement: This research was funded by the Project of Civil Aerospace Advanced Research (Grant No. D010103), Major Project of High Resolution Earth Observation System (Construction and Application Technology of GF-7 Satellite Elevation Datum Conversion Model, Grant No. 42-Y20A09-9001-17/18), Open Funding of the Key Laboratory of Surveying and Mapping Science and Geospatial Information Technology of Ministry of Natural Resources (Grant No. 201907), the Operation and Maintenance Project of Land Satellite Remote Sensing Application System, MNR (Grant No. AB1901), and the Key Laboratory of the Geospace Environment and Geodesy, Ministry of Education, Wuhan University (Grant No. 18-01-05).

Acknowledgments: The European Space Agency is acknowledged for kindly providing the GOCE gravitational gradients. The Technical University of Denmark is acknowledged for kindly providing the DTU13 gravity anomalies.

References

- Andersen, O., Knudsen, P., Kenyon, S., and Holmes, S.: Global and arctic marine gravity field from recent satellite altimetry (DTU13), 76th EAGE Conference and Exhibition 2014, 2014, 1-5,
- Andersen, O. B., Jain, M., and Knudsen, P.: The impact of using Jason-1 and Cryosat-2 geodetic mission altimetry for gravity field modeling, in: IAG 150 Years, Springer, 205-210, 2015.
- Arabelos, D., and Tscherning, C. C.: Calibration of satellite gradiometer data aided by ground gravity data, *Journal of Geodesy*, 72, 617-625, 10.1007/s001900050201, 1998.
- Baur, O., Sneeuw, N., and Grafarend, E. W.: Methodology and use of tensor invariants for satellite gravity gradiometry, *Journal of Geodesy*, 82, 279-293, 10.1007/s00190-007-0178-5, 2008.
- Bouman, J., and Koop, R.: Geodetic Methods for Calibration of GRACE and GOCE, *Space Science Reviews*, 108, 293-303, 10.1023/A:1026127409015, 2003.
- Bouman, J., Koop, R., Tscherning, C. C., and Visser, P.: Calibration of GOCE SGG data using high–low SST, terrestrial gravity data and global gravity field models, *Journal of Geodesy*, 78, 124-137, 10.1007/s00190-004-0328-5, 2004.
- Bouman, J., Rispens, S., Gruber, T., Koop, R., Schrama, E., Visser, P., Tscherning, C. C., and Veicherts, M.: Preprocessing of gravity gradients at the GOCE high-level processing facility, *Journal of Geodesy*, 83, 659-678, 10.1007/s00190-008-0279-9, 2009.



- 349 Bouman, J., Fiorot, S., Fuchs, M., Gruber, T., Schrama, E., Tscherning, C., Veicherts, M., and Visser, P.: GOCE
350 gravitational gradients along the orbit, *Journal of Geodesy*, 85, 791-805, 10.1007/s00190-011-0464-0, 2011.
- 351 Bouman, J., and Fuchs, M. J.: GOCE gravity gradients versus global gravity field models, *Geophysical Journal*
352 *International*, 189, 846-850, 10.1111/j.1365-246X.2012.05428.x, 2012.
- 353 Bouman, J., Ebbing, J., Fuchs, M., Sebera, J., Lieb, V., Szwillus, W., Haagmans, R., and Novak, P.: Satellite
354 gravity gradient grids for geophysics, *Scientific reports*, 6, 1-11, 10.1038/srep21050, 2016.
- 355 Colombo, O. L.: Numerical methods for harmonic analysis on the sphere, Department of Geodetic Science and
356 Surveying, The Ohio State University, Columbus, Ohio, 1981.
- 357 Denker, H.: Computation of Gravity Gradients Over Europe for Validation/Calibration of GOCE Data,
358 Proceedings of the 3rd Meeting of the International Gravity and Geoid Commission Thessaloniki, 2002,
- 359 Drinkwater, M. R., Haagmans, R., and Muzi, D.: The GOCE gravity mission: ESA's first core Earth explorer,
360 Proceedings of the 3rd international GOCE user workshop, 2006, 2006.
- 361 ESA: GOCE Level 2 Product Data Handbook, ESA Document GO-MA-HPF-GS-0110, 2014.
- 362 Eshagh, M.: Least-squares modification of extended Stokes' formula and its second-order radial derivative for
363 validation of satellite gravity gradiometry data, *Journal of Geodynamics*, 49, 92-104, 10.1016/j.jog.2009.11.003,
364 2010.
- 365 Eshagh, M.: Semi-stochastic modification of second-order radial derivative of Abel–Poisson's formula for
366 validating satellite gravity gradiometry data, *Advances in Space Research*, 47, 757-767,
367 10.1016/j.asr.2010.10.003, 2011.
- 368 Fuchs, M. J., and Bouman, J.: Rotation of GOCE gravity gradients to local frames, *Geophysical Journal*
369 *International*, 187, 743-753, 10.1111/j.1365-246X.2011.05162.x, 2011.
- 370 Kern, M.: An analysis of the combination and downward continuation of satellite, airborne and terrestrial gravity
371 data, University of Calgary, Department of Geomatics Engineering, 2003.
- 372 Kern, M., and Haagmans, R.: Determination of gravity gradients from terrestrial gravity data for calibration and
373 validation of gradiometric GOCE data, Springer Berlin Heidelberg, 2005.
- 374 Lu, B., Luo, Z., Zhong, B., Zhou, H., Flechtner, F., Förste, C., Barthelmes, F., and Zhou, R.: The gravity field
375 model IGGT_R1 based on the second invariant of the GOCE gravitational gradient tensor, *Journal of Geodesy*,
376 92, 561-572, 10.1007/s00190-017-1089-8, 2018.
- 377 Pail, R.: In-orbit Calibration and Local Gravity Field Continuation Problem, Egs General Assembly Conference,
378 2002,
- 379 Pavlis, N. K., Holmes, S. A., Kenyon, S. C., and Factor, J. K.: An earth gravitational model to degree 2160:
380 EGM2008, EGU general assembly, 10, 13-18, 2008.
- 381 Rummel, R., Yi, W., and Stummer, C.: GOCE gravitational gradiometry, *Journal of Geodesy*, 85, 777-790,
382 10.1007/s00190-011-0500-0, 2011.
- 383 Siemes, C.: Improving GOCE cross-track gravity gradients, *Journal of Geodesy*, 92, 33-45, 10.1007/s00190-017-
384 1042-x, 2018.
- 385 Šprlák, M., Hamáčková, E., and Novák, P.: Alternative validation method of satellite gradiometric data by integral
386 transform of satellite altimetry data, *Journal of Geodesy*, 89, 757-773, 10.1007/s00190-015-0813-5, 2015.



- 387 van der Meijde, M., Pail, R., Bingham, R., and Floberghagen, R.: GOCE data, models, and applications: A review,
388 International journal of applied earth observation and geoinformation, 35, 4-15, doi:10.1016/j.jag.2013.10.001,
389 2015.
- 390 Veichert, M., Tscherning, C., and Bouman, J.: Improved Cal/Val of GOCE gravity gradients using terrestrial
391 data, Proceedings GOCE User Workshop 2011, ESA SP-696, 2011.
- 392 Wolf, K., and Denker, H.: Upward continuation of ground data for GOCE calibration/validation purposes, Gravity,
393 Geoid and Space Missions, 2005.
- 394 Yildiz, H.: A study of regional gravity field recovery from GOCE vertical gravity gradient data in the Auvergne
395 test area using collocation, Studia Geophysica et Geodaetica, 56, 171-184, 10.1007/s11200-011-9030-8 2012.
- 396 Yildiz, H., Forsberg, R., Tscherning, C. C., Steinhage, D., Eagles, G., and Bouman, J.: Upward continuation of
397 Dome-C airborne gravity and comparison with GOCE gradients at orbit altitude in east Antarctica, Studia
398 Geophysica Et Geodaetica, 61, 53-68, 10.1007/s11200-015-0634-2, 2016.

399